

Triadic Concept Analysis for Logic Interpretation of Simple Artificial Networks

Ingo Schmitt^[0000-0002-4375-8677]

Brandenburgische Technische Universität Cottbus-Senftenberg, Germany
schmitt@b-tu.de
<https://www.b-tu.de/fg-dbis>

Abstract. An artificial neural network (ANN) is a numerical method used to solve complex classification problems. Due to its high classification power, the ANN method often outperforms other classification methods in terms of accuracy. However, an ANN model lacks interpretability compared to methods that use the symbolic paradigm. Our idea is to derive a symbolic representation from a simple ANN model trained on minterm values of input objects. Based on ReLU nodes, the ANN model is partitioned into cells. We convert the ANN model into a cell-based, three-dimensional bit tensor. The theory of Formal Concept Analysis applied to the tensor yields concepts that are represented as logic trees, expressing interpretable attribute interactions. Their evaluations preserve the classification power of the initial ANN model.

Keywords: interpretation · artificial neural network · Formal Concept Analysis · logic

1 Introduction

Besides good accuracy, a classification model should be interpretable. An artificial neural network model, or ANN model, provides good accuracy for many classification tasks but has low interpretability. Numerical methods like an ANN model hide internal decision logic, resulting in a lack of trust [13,9]. Therefore, an ANN is often called a black-box solution.

Interpretability of a classification model is a key requirement in critical applications such as medical diagnosis or decisions that have a strong impact on human life. A task related to interpretation is to explain the classification result for a given input object.

Many researchers, such as those cited in [10,14], strive to make the black-box behavior of an ANN model more transparent and comprehensible. Most of these methods are not based on logic. For example, the Shapley value [22] and its adaptation SHAP [12] compute the importance of single input attributes as part of an additive measure. The SHAP approach generalizes the local interpretable model-agnostic explanations (LIME) [16]. Another proposal is to extract ridge and shape functions in the context of an extracted generalized additive model to illustrate the effect of attributes. Approaches to measuring the importance

of an input attribute can be generalized to measure the strength of interactions among several attributes; see, for example, [15].

Note that decision tree classifiers including their derivatives [23] and the Tsetlin machine [8] are based on Boolean logic decisions. Logic expressions, in general, are seen as much easier to interpret than numerical (sometimes called subsymbolic) classifiers like ANN models. The work from [2,6,3] is an early attempt to bridge neural networks (subsymbolic paradigm) with logic (symbolic paradigm). It defines schemata representing states of a neural network and fuzzy-logic-like operations (conjunction and disjunction). However, these operations do not obey the laws of Boolean algebra.

The work in [7] discusses the concepts of 'incompatibility' and 'implementation' in the context of bridging the symbolic and subsymbolic paradigms of information processing and relates both paradigms to the concepts of quantum mechanics.

An interesting approach [1,25] to bridge logic in the form of decision trees with a deep neural network is to simulate a decision tree using a neural network. After learning and combining the binnings of attribute values, linear networks are trained for every binning combination in order to learn the classification model. In contrast, in our work, the starting point is a given trained simple ANN model, which we attempt to interpret *after* training. Furthermore, the partitioning in [1,25] is based on decision tree split nodes simulated by the softmax function, whereas in our approach, it is based on ReLU nodes.

The main idea of our method is to map a trained ANN model to non-Boolean logic trees by leveraging probability theory, Formal Concept Analysis, and the quantum-logic-inspired decision tree (QLDT [21]). We obtain a linear combination of logic trees that helps to interpret the semantics of a given ANN model. This approach resembles the RuleFit method [4], which relies on a linear combination of rules derived from decision trees. However, decision trees are based on Boolean logic and lack smoothness with respect to continuous input values.

For our interpretation method, we define some restrictions attributed to a one-class ANN classifier model already trained using balanced training data TR , both of which are the starting point for us:

- The ANN consists of linear layers (such as convolution, average pooling, and fully connected layers), one layer containing exclusively ReLU nodes, and one output node.
- The target output of the classification is 1 for the class decision and 0 otherwise. The target value is obtained by applying a threshold operator τ on the output node.
- The number $\#atts$ of input object attributes is small. The values of every attribute lie within the unit interval $[0, 1] \in \mathbb{R}$, expressing the degree of fulfillment of a human-understandable property. For example, see the left part of Table 1 with two training objects $(x_1, y_1), (x_2, y_2)$ and two attributes a_1, a_2 with the attribute values $x_i[1], x_i[2]$.
- The ANN has $2^{\#atts}$ input nodes for the minterm values (defined below) of an input object.

Table 1. Two example objects $(x_1, y_1), (x_2, y_2)$ over two attributes a_1, a_2 with $x_i = (x_i[1], x_i[2])$ (left part) and four derived minterms (right part): $mt_i[0] = (1 - x_i[1]) \cdot (1 - x_i[2])$, $mt_i[1] = (1 - x_i[1]) \cdot x_i[2]$, $mt_i[2] = x_i[1] \cdot (1 - x_i[2])$, $mt_i[3] = x_i[1] \cdot x_i[2]$

object i	attr. values		target y_i	derived minterms			
	$x_i[1]$	$x_i[2]$		$mt_i[0]$	$mt_i[1]$	$mt_i[2]$	$mt_i[3]$
1	0.8	0.1	1	0.18	0.02	0.72	0.08
2	0.5	0.6	0	0.2	0.3	0.2	0.3

For a logical interpretation of an ANN model, we require $2^{\#atts}$ minterm values $mt_i[k]$ instead of $\#atts$ values $x_i[j]$ as input. Minterm values are conjunctions (expressed as products) of negated ($1 - x_i[j]$) and non-negated attribute values $x_i[j]$. Each minterm value expresses a specific interaction among all attributes. In accordance with [21,20], we define:

$$mt_i[k] := \prod_{j=1}^{\#atts} (1 - x_i[j])^{1-b_j} \cdot x_i[j]^{b_j}$$

where the integer $k = 0, \dots, 2^{\#atts} - 1$ is the minterm identifier and $b = b_1 \dots b_{\#atts}$ is the bit code of k ($k = \sum_{j=0}^{\#atts-1} b_{\#atts-j} \cdot 2^j$). It can be shown that $\sum_k mt_i[k] = 1$ holds. For example, see the right part of Table 1 for the 2^2 minterm values $mt_i[k]$.

As a result of our method, we obtain logic trees. Three very simple examples, along with their arithmetic evaluations, are depicted in Figure 1. We will describe such logic trees in more detail later.

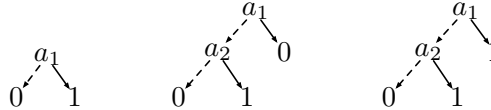


Fig. 1. Example logic trees: solid lines refer to non-negated attribute evaluations, while dashed lines refer to negated attribute evaluations. Arithmetic evaluations of the logic trees are as follows: $[a_1]^i = x_i[1]$ (left), $[\bar{a}_1 \wedge a_2]^i = (1 - x_i[1]) \cdot x_i[2]$ (middle), and $[a_1 \vee (\bar{a}_1 \wedge a_2)]^i = x_i[1] + (1 - x_i[1]) \cdot x_i[2]$ (right).

2 ANN Partition Cells

A ReLU node in an ANN is defined by the function

$$ReLU(z) = \begin{cases} z & \text{if } z \geq 0 \\ 0 & \text{otherwise.} \end{cases}$$

Let us assume the given ANN model has l ReLU nodes, denoted as $ReLU_1, \dots, ReLU_l$. For every input object, the status of a ReLU node is either *active*, corresponding

to the identity function, or *inactive*, corresponding to the zero function. In the following, we will denote the status of an active ReLU node by the bit 1 and an inactive node by the bit 0. Because of the linear layers below a ReLU node, its status separation between active and inactive corresponds to a hyperplane in the input space $[0, 1]^{2^{\#atts}}$.

For an input object x_i , let us interpret the sequence of status bits of all l ReLU nodes as an integer, which we call its *partition number* p_i . We define $active(p)$ as the set of active ReLU nodes for a given partition number p . Partition numbers identify *partition cells* of the input space $\mathbb{R}^{2^{\#atts}}$: input objects with the same partition number belong to the same partition cell. Since every ReLU node corresponds to a hyperplane, every partition cell induces a convex subset of $\mathbb{R}^{2^{\#atts}}$. All partition cells are mutually disjoint. Because all layers of the ANN model except the ReLU nodes are linear, we can combine the linear layers for a given partition cell p into one linear map mw^p from the input minterm values to the output node value. Here, $mw^p[k]$ denotes the minterm weight for minterm k . An example of linear mappings of partition cells over 2^2 minterms is given in Table 2.

Table 2. Example values $mw^p[k]$ for 2^2 minterms $k = 0, \dots, 3$

partition p	minterm weights			
	$mw^p[0]$	$mw^p[1]$	$mw^p[2]$	$mw^p[3]$
1	-8	3	6	2
\vdots	\vdots	\vdots	\vdots	\vdots

For a given ANN model, there are at most 2^l partition cells. If a cell p lies completely outside the input space $[0, 1]^{2^{\#atts}}$, then there is no input object x_i for which $p_i = p$ holds. All partition cells form an atomic, Boolean subset lattice over the respective sets $active(p)$. Figure 2 depicts an example lattice for three ReLU nodes and eight partitions cells.

For every partition cell we use following information:

- Number of training objects i for which $p_i = p$
- Number of 1-objects and number of 0-objects with $p_i = p$
- Minterm weights: mw^p

Based on this information, not all partition cells are essential for interpreting an ANN model. Cells with no assigned training objects or cells containing only 1-objects or only 0-objects are of low relevance, as they do not contribute to separating input objects. Cells with many training objects and a balanced occurrence of 1-objects and 0-objects are of high relevance.

As a result of our ANN architecture, all minterm weights of a partition cell can be derived by summing the weights from its respective atomic partition cells. A

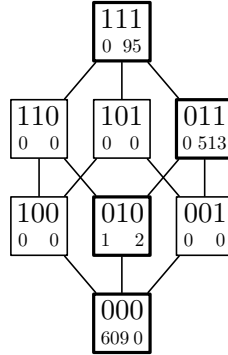


Fig. 2. Example lattice of partition cells identified by bit codes for the status of three ReLU nodes: the small number on the left indicates the number of zero-objects ($y_i = 0$), and the small number on the right indicates the number of one-objects ($y_i = 1$) in TR . Bold partitions are those that are of interest (non-empty).

partition cell is considered atomic if exactly one ReLU node is active:

$$mw^p = \sum_{i:b_i=1} mw^{2^{l-i}}$$

where $b_1 b_2 \dots b_l$ is the bit code of partition cell number p . An example derivation is $mw^{101} := mw^{100} + mw^{001}$. This derivation is very useful because only the minterm values of atomic partition cells — namely, $l \cdot 2^{\#atts}$ values — need to be stored. In the following sections, we assume P to be the set of essential partition cells.

3 Converting Minterm Weights to a Bit Tensor

Let the minterm weights $mw^p[k]$ for all partition cells $p \in P$ over the minterms k be given, as shown for example in Table 2. The input for the ANN model is an object x_i with minterm values $mt_i[k]$ for every minterm k and the assigned partition cell $p = p_i$, as shown for example in Table 1. The score $\text{ANN}(x_i)$ can be written as the scalar product $\text{ANN}(x_i) := \langle mt_i, mw^p \rangle = \sum_k mt_i[k] \cdot mw^p[k]$. For example, using the objects in Table 1 with $p_1 = p_2 = 1$ and the minterm weights in Table 2, we obtain the scores $\text{ANN}(x_1) = 3.1$ and $\text{ANN}(x_2) = 1.1$.

If we assume different score values for all objects, their scores can be strictly ordered. For our interpretation method, we convert the minterm weights $mw^p[k]$ into bit values by applying a strictly monotonic increasing linear function f to them. Since the scalar product is linear in its arguments, applying f to the minterm weights preserves the strict order of the objects:

$$\begin{aligned} \langle mt_i, f(mw^p) \rangle &= f(\langle mt_i, mw^p \rangle) \\ \langle mt_{i_1}, mw^p \rangle &> \langle mt_{i_2}, mw^p \rangle \Leftrightarrow f(\langle mt_{i_1}, mw^p \rangle) > f(\langle mt_{i_2}, mw^p \rangle) \end{aligned}$$

As consequence, the application of the modified threshold $f(\tau)$ to the scores $f(\text{ANN}(x_i))$ preserves the original class decisions.

Next, we remove the fractional part from the mapped minterm values $f(mw^p[k])$ and encode the remaining integer as a binary number of $\#bits$ bits. This removal of the fractional part introduces a truncation error. Consequently, if we apply the truncated minterm weights to the input objects, objects with different scores might receive the same scores, which means the strict score ordering becomes a weak order.

To determine the linear function f , we derive a minterm value interval $[a, b]$ with $a = \min_{p \in P, k} mw^p[k]$ and $b = \max_{p \in P, k} mw^p[k]$. We encode every minterm weight $v := mw^p[k]$ as an integer v' with $\#bits$ bits:

$$v' := \lfloor f(v) \rfloor := \left\lfloor \frac{v - a}{b - a} * \frac{2^{\#bits}}{1 + \epsilon} \right\rfloor \in \{0, 1, \dots, 2^{\#bits} - 1\}. \quad (1)$$

The denominator $1 + \epsilon$, where ϵ is a small value, e.g. $2^{-(\#bits+4)}$, is necessary to obtain $2^{\#bits} - 1$ instead of $2^{\#bits}$ for $v := b$. The mapping is depicted in Figure 3.

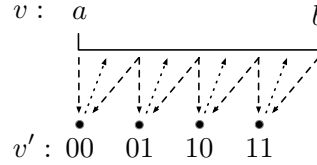


Fig. 3. Dashed lines: lossy mapping of minterm weights to binary numbers ($\#bits = 2$); dotted lines: reconstruction function

Table 3 shows the mapping of our introduced example minterm weights. If we apply the mapped minterm values to the example objects in Table 1, we obtain the scores $\text{ANN}(x_1)' = 2.38$ and $\text{ANN}(x_2)' = 2.1$.

Table 3. Mapped values $mw^p[k]$ from Table 2 over all minterms $k = 0, \dots, 3$ of partition $p = 1$ with $\#bits = 2$; the last two rows show bit values of $\lfloor f(mw^p[k]) \rfloor$ with respect to the two bit levels

	Minterms k			
	0	1	2	3
$mw^p[k]$	-8	3	6	2
$f(mw^p[k])$	0	3.14	3.99	2.85
$\lfloor f(mw^p[k]) \rfloor$	0	3	3	2
$bl = 0 : 2^0$	0	1	1	0
$bl = 1 : 2^1$	0	1	1	1

Next, we define a linear reconstruction function that attempts to reconstruct v from v' with a small average reconstruction error. The linear reconstruction function for obtaining v'' from v' , where $v'' \approx v$, is given as:

$$v'' := \left(v' * \frac{1 + \epsilon}{2^{\#bits}} + 2^{-(\#bits+1)} \right) * (b - a) + a. \quad (2)$$

To achieve a small reconstruction error, the term $2^{-(\#bits+1)}$ selects the middle of the truncation interval, as shown in Figure 3. If we assume a uniform distribution for the minterm values, the average reconstruction error is:

$$E(|v - v''|) = \frac{b - a}{2^{\#bits+2}}$$

and the upper bound is:

$$|v - v''| \leq \frac{b - a}{2^{\#bits+1}}.$$

Since the reconstruction error decreases exponentially with the number of bits, the parameter $\#bits$ can be small to ensure a small reconstruction error.

After mapping all minterm values, the class decision threshold τ needs to be mapped as well. The truncation of the minterm values produces an average error of $1/2$ on the score values. Thus, we choose $\tau' = f(\tau) - 1/2$.

In our example, we assume the initial value $\tau = 2$ and obtain $\tau' = 2.36$. As a result, the threshold τ' effectively separates object x_1 from x_2 after the minterm weight mappings ($\text{ANN}(x_1) = 3.1$, $\text{ANN}(x_2) = 1.1$, and $\text{ANN}(x_1)' = 2.38$, $\text{ANN}(x_2)' = 2.1$).

The values $v' = \lfloor f(mw^p[k]) \rfloor$ are regarded as binary numbers. For our example, see the last two rows in Table 3. Every bit derived from a trained ANN model depends on the combination of a partition cell $p \in P$, a minterm $k \in \{0, 1, \dots, 2^{\#atts} - 1\}$, and a bit level $bl \in \{0, 1, \dots, \#bits - 1\}$:

$$bt(p, k, bl) := \lfloor f(mw^p[k]) \rfloor \& 2^{bl}$$

where bt is a three-dimensional bit tensor and ' $\&$ ' denotes the bitwise **and**. As a result, the semantics of an ANN model can be approximated by a three-dimensional tensor $bt[p, k, bl]$ of bit values.

From this construction, we can formalize the approximation of $f(\text{ANN}(x_i))$ for an input object x_i with $p_i = p$ as:

$$f(\text{ANN}(x_i)) = \sum_{k=0}^{2^{\#atts}-1} mt_i[k] \cdot f(mw^p[k]) \approx \sum_{k=0}^{2^{\#atts}-1} mt_i[k] \cdot \lfloor f(mw^p[k]) \rfloor$$

and

$$\begin{aligned} \sum_{k=0}^{2^{\#atts}-1} mt_i[k] \cdot \lfloor f(mw^p[k]) \rfloor &= \sum_{k=0}^{2^{\#atts}-1} mt_i[k] \cdot \sum_{bl=0}^{\#bits-1} bt(p, k, bl) \cdot 2^{bl} \\ &= \sum_{bl=0}^{\#bits-1} 2^{bl} \cdot \sum_{k=0}^{2^{\#atts}-1} mt_i[k] \cdot bt(p, k, bl) \end{aligned}$$

From a given bit tensor bt , we compute its energy:

$$power(bt) := \sum_{p \in P} \sum_{k:=0}^{2^{\#atts}-1} \sum_{bl:=0}^{2^{\#bits}-1} bt[p, k, bl] \cdot 2^{bl} = \sum_{p \in P} \sum_{k:=0}^{2^{\#atts}-1} \lfloor f(mw^p[k]) \rfloor.$$

The energy can be understood as the contribution of all bit-encoded minterm weights across all partition cells. It approximates the sum of all minterm weights of the given ANN model.

4 Formal Concept Analysis and Triadic Concept Analysis

Formal Concept Analysis (FCA) is a theory developed by Ganter and Wille [11,5,24]. In our method, we use FCA to convert the tensor bt into a compact representation, which we later interpret as logic trees.

Formal Concept Analysis is based on a binary relation, whereas Triadic Concept Analysis (TCA) can be seen as its generalization to a ternary relation. In the following, we define the main FCA components: A *dyadic context* is a triple (G, M, I) where G is a set of objects and M is a set of attributes¹. $I \subseteq G \times M$ is a binary relation over G and M . $(g, m) \in I$, also written as gIm , indicates that an object g of G has a certain attribute m of M . A context can be visualized as a cross table, see for example Table 4 left, where a cross means $gIm := (g, m) \in I$. Columns refer to objects, and rows refer to attributes. We define for a subset $A \subseteq G$ the function $' : 2^G \rightarrow 2^M$ as $A' := \{m \in M | gIm \text{ for all } g \in A\}$. Analogously, we define for a subset $B \subseteq M$ the function $' : 2^M \rightarrow 2^G$ as $B' := \{g \in G | gIm \text{ for all } m \in B\}$. Based on these functions, a *concept* of a context is a pair (A, B) with $A \subseteq G, B \subseteq M, A' = B$, and $B' = A$. In other words, $A \times B \subseteq I$ (cross-product rule) holds, and A as well as B cannot be extended without violating the cross-product rule. If we depict a context as a cross table, then a concept (A, B) corresponds to a maximal rectangle filled with crosses for some permutation of columns and rows, see for example the first concept in Table 4.

Table 4. Example context and some concepts; bold crosses correspond to the first concept

			g_1	g_2	g_3
m_1			\times		
m_2			\times	\times	
m_3	\times	\times	\times		

$concepts = \left\{ \begin{array}{l} (\{g_2, g_3\}, \{m_2, m_3\}) \\ (\{g_1, g_2, g_3\}, \{m_3\}) \\ (\{g_2\}, \{m_1, m_2, m_3\}) \end{array} \right\}$

For a given context, up to $2^{\min\{|G|, |M|\}}$ concepts can exist. All concepts together form a Boolean subset lattice over the partially ordered set $(\{(A'', A') | A \subseteq$

¹ The terms 'object' and 'attribute' are abstract and do not refer to the input objects and their attribute values in our classification task.

$G\}, \leq)$ with $(A''_1, A'_1) \leq (A''_2, A'_2) \Leftrightarrow A''_1 \subseteq A''_2$. Concepts can overlap, e.g., $(\{g_2\}, M)$ and $(G, \{m_3\})$ overlap with $g_2 \in m_3$, meaning they can share crosses.

We derive a set **concepts** (which does not necessarily contain all concepts) from singleton sets as follows:

$$\text{concepts} := \{(\{a\}'', \{a\}') | a \in G\} \cup \{(\{b\}', \{b\}'') | b \in M\}.$$

This results in no more than $|G| + |M|$ concepts. Note that every cross $(g, m) \in I$ is covered by at least one concept from **concepts**.

Let us now generalize Formal Concept Analysis to Triadic Concept Analysis (TCA): A *triadic context* is a quadruple (K_1, K_2, K_3, Y) where K_1 is a set of objects, K_2 is a set of attributes, and K_3 is a set of conditions. $Y \subseteq K_1 \times K_2 \times K_3$ is a ternary relation over K_1 , K_2 , and K_3 . The expression $(g, m, b) \in Y$ means that object g has attribute m under condition b . We define for a triadic context, $X_2 \subseteq K_2$, and $X_3 \subseteq K_3$, the function ${}^1 : 2^{K_2} \times 2^{K_3} \rightarrow 2^{K_1} : (X_2, X_3)^1 := \{x_1 \in X_1 | (x_1, x_2, x_3) \in Y \text{ for all } (x_2, x_3) \in X_2 \times X_3\}$. Analogously, we define the functions $(X_1, X_3)^2$ and $(X_1, X_2)^3$ for computing X_2 and X_3 , respectively. A *triadic concept* is a triple (X_1, X_2, X_3) for which $X_1 = (X_2, X_3)^1$, $X_2 = (X_1, X_3)^2$, and $X_3 = (X_1, X_2)^3$ hold. A triadic concept can be seen as a maximal cuboid fulfilling the cross-product rule $X_1 \times X_2 \times X_3 \subseteq Y$. From the definition, we see that a triadic concept is uniquely defined for two given sets X_i, X_j . From a given triadic context (K_1, K_2, K_3, Y) , we compute triadic concepts **triconcepts** slice-wisely by:

$$\text{triconcepts} := \bigcup_{x_1 \in K_1} \{(X_2, X_3)^1, X_2, X_3 | (X_2, X_3) \in \text{concepts}^{x_1}\},$$

where concepts^{x_1} are the dyadic concepts **concepts** computed from the x_1 -slice dyadic context (G, M, I) derived from the triadic context: $(x_2, x_3) \in I \Leftrightarrow (x_1, x_2, x_3) \in Y$ and $G := K_2, M := K_3$.

5 Generating Logic Trees from Exclusive Triconcepts

In Section 3, we derived a three-dimensional tensor bt from an ANN model. We interpret it as a triadic context (K_1, K_2, K_3, Y) with $K_1 = P$, $K_2 = \{0, 1, \dots, 2^{\#atts} - 1\}$, $K_3 = \{0, 1, \dots, \#bits - 1\}$, and $Y = \{(p, k, bl) | bt[p, k, bl] = 1\}$. For example, we can regard the last two rows of Table 3 of the partition p as a triadic context: $K_1 = \{p\}$, $K_2 = \{0, 1, 2, 3\}$, $K_3 = \{0, 1\}$, and

$$Y = \{(p, 1, 0), (p, 2, 0), (p, 1, 1), (p, 2, 1), (p, 3, 1)\}.$$

We compute triadic concepts as $\{c_j(X_1, X_2, X_3)\} := \text{triconcepts}$. From our example in Table 3, we obtain two concepts: $c_1 := c_1(\{p\}, \{1, 2, 3\}, \{1\})$ and $c_2 := c_2(\{p\}, \{1, 2\}, \{0, 1\})$. A concept can be seen as a maximal cuboid completely filled with set bits. Analogous to the energy of a context, we now define the *energy* of a concept c_j as the product of the number of its partition cells, the

number of its minterms, and the *powersum* := $\sum_{x_3 \in X_3} 2^{x_3}$ over its bit code levels:

$$power(c_j(X_1, X_2, X_3)) := |X_1| * |X_2| * \sum_{x_3 \in X_3} 2^{x_3}$$

The energy of our two example concepts is: $power(c_1) = power(c_2) = 6$. In combination with the context energy, we define the *relative concept energy* as $relpower(c) := power(c)/power(bt)$ ².

We will interpret the minterms X_2 of a triadic concept as a logic expression with a relative power value computed from X_3 and valid for objects of the partition cells in X_1 . As mentioned in the previous section, the cuboids of different triadic concepts can overlap and would produce overlapping logic expressions. Our aim is to obtain non-overlapping logic expressions with high energy. Therefore, we compute an array ex_c of exclusive triadic concepts ordered by descending relative energy from a triadic context. Thus, $\sum_{xc \in ex_c} relpower(xc) = 1$ holds, or in other words, every set bit of bt is contained in exactly one exclusive triadic concept xc . See Algorithm 4 for computing the required array ex_c . From our example in Table 3 we obtain: $ex_c[0] = c_0(\{p\}, \{1, 2\}, \{0, 1\})$ with $power(ex_c[0]) = 6$ and $ex_c[1] = c_1(\{p\}, \{3\}, \{1\})$ with $power(ex_c[1]) = 2$.

```

1  function excl_triconcepts(tricontext bt): array of triconcepts
2    ex_triconcepts := []      // empty result array
3    C := triconcepts(bt)
4    xc:=arg maxc ∈ C relpower(c) // concept with highest power
5    ex_triconcepts.append(xc)
6    // reduce triicontext by concept with highest power
7    for x1 ∈ xc.X1
8      for x2 ∈ xc.X2
9        for x3 ∈ xc.X3
10       bt[x1,x2,x3] := 0 // no cross
11     if power(bt) > 0 // is triicontext non-empty
12     go to line 3
13   return ex_triconcepts

```

Fig. 4. Extracting exclusive triconcepts

In the algorithm, we used *relpower* in Line 4 to find the best triadic concept. However, this is only the first of four possible methods:

1. M1: relative power ($\#partitions * \#minterms * powersum$)
2. M2: $\#partitions * powersum$
3. M3: *powersum*

² Alternatively, we can use the number of *TR* objects (support) of the covered partition cells instead of the number $|X_1|$ of cells for both energy formulas.

4. M4: accuracy across the objects of the covered partition cells

We will compare their impacts on the logic tree generation in Section 7.

A set X_2 of minterm identifiers from a triadic concept $c_j(X_1, X_2, X_3)$ is not an intuitive representation of a logic expression. Therefore, we construct a quantum-logic-inspired decision tree (QLDT [21]) from X_2 and present it to the expert for interpretation. The QLDT is a compact representation of a logic expression defined by X_2 . The main construction idea is to use the bit codes of active and inactive minterms

$$\{(bit\text{-}code}(k), 1) | k \in X_2\} \cup \{(bit\text{-}code}(k), 0) | k \in K_2 \setminus X_2\}$$

as training data for learning a classical decision tree. The bits of the bit code for minterm k represent all n original attributes, either negated or non-negated. The attributes near the root of the resulting decision tree are more effective at separating active from inactive minterms than those further away.

From the example triadic concept $ex_c[0]$ with $X_2 = \{1, 2\}$ we obtain training data: $\{(00, 0), (01, 1), (10, 1), (11, 0)\}$. The *powersum* derived from X_3 is $2^0 + 2^1 = 3$. The final logic tree is depicted in Figure 5.

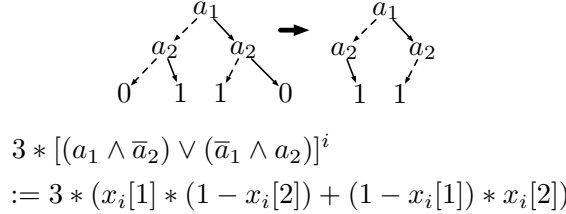


Fig. 5. Example logic tree for $ex_c[0]$; solid lines non-negated and dashed line means negated evaluation, paths to 0-leaves can be dropped; below the arithmetic evaluation for an object x_i (discussed in Section 6)

Figure 6 depicts the logic tree from $ex_c[1]$ with $X_2 = \{3\}$, training data $\{(00, 0), (01, 0), (10, 0), (11, 1)\}$ and *powersum* $2^1 = 2$.

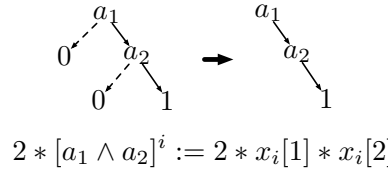


Fig. 6. Example logic tree for $ex_c[1]$; solid lines non-negated and dashed line means negated evaluation, paths to 0-leaves can be dropped; below the arithmetic evaluation for an object x_i

6 Evaluation and Interpretation of Logic Trees

The minterms of a triadic concept can be seen as minterms of a logic expression in disjunction normal form. Since the minterm values of the input objects are continuous, the evaluation of a logic expression following our method is not based on Boolean values. However, as proven in [18,19], the underlying commuting quantum logic obeys the rules of Boolean algebra and probability theory on statistically independent attribute values. The evaluation result is a continuous score value that is mapped to a class decision using a threshold operator (a step function) τ .

A logic tree is a compact representation of a logic expression based on minterms that provides good interpretability. An inner tree node branches on a single attribute, where every edge to a child corresponds either to the negated or the non-negated attribute evaluation. Similar to decision trees, leaves refer to class decisions. For our one-class classification problem, we ignore 0-leaves and focus on 1-leaves only.³ Let L_1 be the set of all paths from the root to a 1-leaf. All literals on a given path $l \in L_1$, negated or non-negated, are combined conjunctively. Every attribute of an L_1 -path can occur only once. The branching of an inner node based on an attribute to two children, one negated and the other non-negated, corresponds to an exclusive disjunction.

Following the rules of probability theory, we evaluate a logic tree using three rules:

1. The probability value of a negated event is computed by subtracting it from 1.
2. The probability value of a conjunction of independent events is computed by the arithmetic product.
3. The probability value of an exclusive disjunction is computed by the arithmetic sum.

As a result, we obtain the evaluation of a logic tree $qldt$ against an object x_i as $[qldt]^i := \sum_{l \in L_1} \prod_{e_{lj} \in \text{path}(l)} [e_{lj}]^i$, where $[e_{lj}]^i := x_i[j]$ holds for a non-negated attribute a_j and $[e_{lj}]^i := 1 - x_i[j]$ holds for a negated one. Let us assume a special input object where only values 0 and 1 occur as attribute values. In that case, the $qldt$ evaluation coincides with Boolean logic. Thus, our evaluation formula $[qldt]^i$ can be seen as a generalization of Boolean logic.

From several exclusive concepts, we obtain several logic trees. To evaluate an input object x_i , we choose the logic trees for concepts that cover the object:

$$QLDT(i) = \{qldt(c) | c \in \text{excl_triconcepts(bt)} \wedge p_i \in c.X_1\},$$

sum their weighted tree evaluations up and obtain the score value:

$$\text{score}(x_i) = \sum_{qldt(c) \in QLDT(i)} \text{powersum}(c) * [qldt(c)]^i.$$

³ Focusing on 0-leaves is the logical negation of focussing on 1-leaves.

If $score(x_i) > \tau'$, then we obtain the class value 1; otherwise, we obtain 0.

Due to our mapping from the bit tensor to the logic trees, we obtain for input object x_i with $p = p_i$ the following equivalence:

$$\sum_{qldt(c) \in QLDT} powersum(c) * [qldt(c)]^i = \sum_{bl=0}^{\#bits-1} 2^{bl} \cdot \sum_{k=0}^{2^{\#atts}-1} mt_i[k] \cdot bt(p, k, bl).$$

For our example objects, the weighted sum over $ex_c[0]$ and $ex_c[1]$ yields the $score(x_1) = 2.38$ and the $score(x_2) = 2.1$. That is, the weighted sum over the logic trees approximates the minterm evaluation.

Interpretation of Minterm Weights and Logic Trees

For interpretation, an expert of the domain and an expert of logic and classification should work together. We will call them below as *expert*.

Based on the minterm weights of a partition cell, we can compute the contribution of individual attributes across the minterms using the Shapley formula [17]:

$$Sh_i = \sum_{S \subseteq N \setminus \{i\}} \frac{(n-1-|S|)!|S|!}{n!} (v(S \cup \{i\}) - v(S)).$$

The main idea is to interpret all non-negated attributes of a minterm as a set. The input for computing the Shapley values are the set of indices $N := \{1, \dots, n\}$ for the object attributes a_1, \dots, a_n and the minterm values $v(S) := mw^p[k]$, where $k = \sum_{i \in S} 2^{i-1}$ is composed of attributes that are regarded as non-negated attributes of minterm k . Please note that v in our case is not necessarily monotonic, and $v(\emptyset) = mw^p[0]$ does not need to be zero. By summing up all Shapley values, we obtain:

$$\sum_i Sh_i = v(N) - v(\emptyset) = mw^p[2^n - 1] - mw^p[0].$$

The Shapley values computed as described above are independent of objects. If we want them to be dependent on an input object x_i , then compute $v(S) := mt_i[k] \cdot mw^p[k]$. A general disadvantage of Shapley values is the lack of showing interactions between attributes.

Our interpretation method derives logic trees from an ANN model and is therefore a model dependent and inherent interpretation method. A logic tree represent complex interactions between attributes for solving a classification problem.

The logic expression behind the tree can be compared with another logic expression that is a hypothesis of the expert. For comparison, the sets of underlying minterms can be analysed on intersections. For example, if every hypothesis minterm is contained in the tree expression, then the hypothesis implies the tree expression. For a deeper discussion, see [21].

If a derived logic tree $qldt(c)$ is too complex for human interpretation, then its individual paths to the leaves $l \in L_1$ can be taken for interpretation. We know from the tree evaluation that the individual path evaluations are simply

summed up. Each individual leaf path can be interpreted as a conjunction of literals. The following properties of a leaf path $l \in L_1$, as part of the tree, are independent of TR and are valuable for interpretation:

- Leaf depth: the depth $depth(l)$ within the tree corresponds to the number of path attributes and tells us how many minterm are covered: $2^{n-depth(l)}$. Here, n is the total number of attributes.
- Weight of the tree: $powersum(c)$
- Number of partition cells: $|c.X_1|$

For a given input object x_i with $p = p_i$, the path evaluation shows its contribution $[l]^i := \prod_{j \in path(l)} [a_{lj}]^i$ to the score. Finally, if we take training (or test) data T , we can compute the average path contribution $\frac{1}{|T|} \sum_{(x_i, target) \in T} [l]^i$ for the value $target = 0$ or $target = 1$ to the scores, as well as values for accuracy, recall, and precision. Examples in an experimental context are given next.

7 Experimental Interpretation of an ANN Model

The experimental dataset is the blood transfusion service center dataset⁴. A classifier needs to be developed to predict whether a person donates blood or not. To make that decision for each person, we have the following information: recency r (months since the last donation), frequency f (total number of donations), monetary status m (total blood donated in c.c.), and time t (months since the first donation). In the balanced case, 178 people donated blood and 178 did not.

We trained an ANN model with 5 ReLU nodes, 16 input nodes, and one output node. The final decision threshold τ is determined by choosing the training score value that achieves the best accuracy. The transfusion problem is a difficult classification problem, and our model yields 74% accuracy. From the network, we derived its partition cells. Figure 7 shows a Hasse diagram of the partially ordered set of its non-empty partition cells. We selected partition cells (1, 5, 17, 20, 28) as essential cells: 305 out of the total 356 people belong to the essential cells.

Table 5. Shapley values of the four attributes computed from the minterms of essential partition cells; the largest absolute values are marked in bold text

partition cell	recency	frequency	monetary	time
1	0.044	-0.026	-0.026	0.008
5	-0.075	0.041	0.032	0.021
17	0.062	0.001	0.008	0.049
20	-0.101	0.095	0.093	0.054
28	0.081	-0.119	0.011	0.005

⁴ <https://archive.ics.uci.edu/ml/datasets.php>

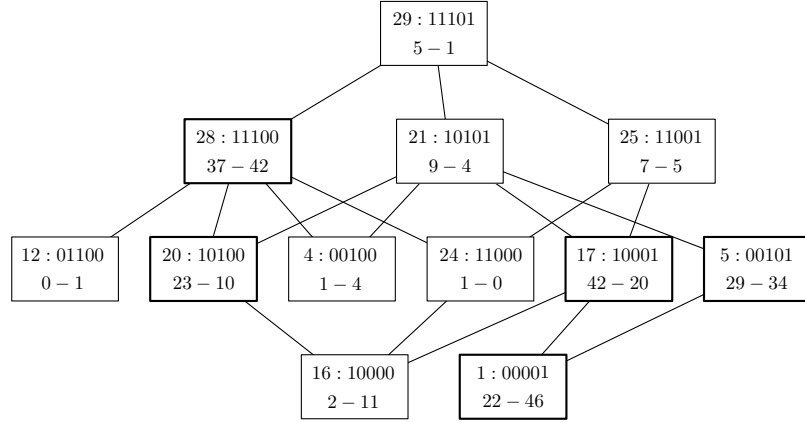


Fig. 7. Transfusion: partially ordered set of non-empty partition cells; bit code shows activity of the ReLU-nodes; subset relation between sets of active ReLU-nodes form a partially ordered set; lower left value shows the number of 1-objects; lower right number shows the number of 0-objects; selected cells (1,5,17,20,28) have high support (sum of lower numbers) and are indicated as bold-lined boxes

Table 5 shows the Shapley values of the essential partition cells. The attribute **time** is positive across all essential partition cells but shows low impact. The attributes **recency** and **frequency** have a high impact; however, they are positive in some partition cells and negative in others. This indicates that these attributes play different roles depending on other attributes (high interactions), and the behavior of people in different cells is not homogeneous.

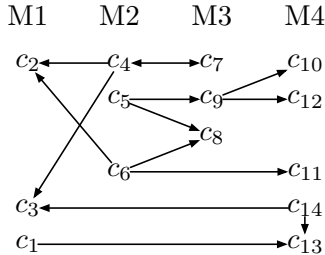


Fig. 8. Transfusion: concepts and their implications (subsets of minterm sets and supersets of partition cell sets)

From the minterm values, we compute the bit tensor with 7 bits. Testing the resulting concepts yields an accuracy of 74%, indicating that the truncation error is small enough. Table 6 shows the top concepts based on different methods of selecting the best concepts. Comparing the concepts derived from different methods reveals implications among them, as illustrated in Figure 8. One concept

Table 6. Top exclusive concepts using methods M1, M2, M3, and M4

concept	partition cells	minterms	bit levels
M1: $\#partitions * \#minterms * powersum$			
c_1	{1, 5, 17}	{0, 2 – 7, 9, 15}	{1}
c_2	{28}	{0 – 2, 4, 8, 9, 11, 13}	{0}
c_3	{20, 28}	{1, 6 – 8, 14, 15}	{1}
M2: $\#partitions * powersum$			
c_4	{5, 20, 28}	{8}	{0, 4}
c_5	{5, 17, 20}	{14}	{0}
c_6	{1, 17, 28}	{1}	{0}
M3: $powersum$			
c_7	{5, 20, 28}	{8}	{0, 4}
c_8	{17}	{1, 14}	{0, 6}
c_9	{5, 20}	{14}	{0, 3}
M4: accuracy			
c_{10}	{20}	{2, 4, 5, 9 – 14}	{5}
c_{11}	{17}	{1, 2, 4, 6 – 13, 15}	{2}
c_{12}	{5}	{2, 4 – 6, 10 – 14}	{3}
c_{13}	{1}	{0, 2 – 9, 14, 15}	{1}
c_{14}	{1, 20, 28}	{6}	{3}

implies another if their minterm sets are in a subset relation and their partition cell sets are in a superset relation. Although concepts c_{13} and c_{14} are exclusive due to their distinct sets of bit levels, concept c_{14} implies concept c_{13} because of the subset relation between their minterm sets.

Next, we examine the properties of the derived top concepts in Table 7 with regard to *relpower*, precision, recall, accuracy, and support (number of covered training objects). There are very specific concepts (c_6, c_{14}) with high precision and low recall, but also very general concepts (c_4, c_7, c_{10}, c_{13}) with high recall and low precision. Due to the method of selecting the best concepts, method M1 concentrates concepts with high *relpower* at the top, whereas method M4 prefers concepts with high accuracy. Ultimately, the expert must decide which method is preferred.

Focusing on M4-concepts, we see that the concepts $c_{10}, c_{11}, c_{12}, c_{14}$ cover all essential partition cells. At the same time, their accuracy values are not less than 70%, which is close to the network's accuracy of 74%. The support is 305 out of the total 356. This means that only four concepts are necessary to approximate the accuracy of the network.

Let us now examine the logic interpretations of the concepts. The concept c_{14} , with just one minterm, is very simple: $\bar{r} \wedge f \wedge m \wedge \bar{t}$. Figure 9 depicts the logic trees of the concepts c_{10} and c_{11} . Since these are hard to interpret, we examine their paths to 1-leaves, as shown in Table 8. For each path, we present precision, recall, accuracy, the number of covered minterms (#mt), and the averaged path evaluations, separated for 0-objects (0-avg) and 1-objects (1-avg). The difference

Table 7. Concept characteristics

concept	relnpower	precision	recall	accuracy	support
c_1	19%	58%	26%	55%	193
c_2	11%	51%	54%	54%	79
c_3	8%	64%	26%	52%	112
c_4	4%	53%	98%	54%	175
c_5	4%	75%	50%	60%	158
c_6	4%	100%	1%	52%	209
c_7	4%	53%	98%	54%	175
c_8	2%	75%	73%	66%	62
c_9	3%	63%	84%	65%	96
c_{10}	0.4%	71%	100%	72%	33
c_{11}	4%	77%	83%	72%	62
c_{12}	1%	76%	55%	71%	63
c_{13}	1%	70%	97%	70%	68
c_{14}	7%	100%	9%	70%	180

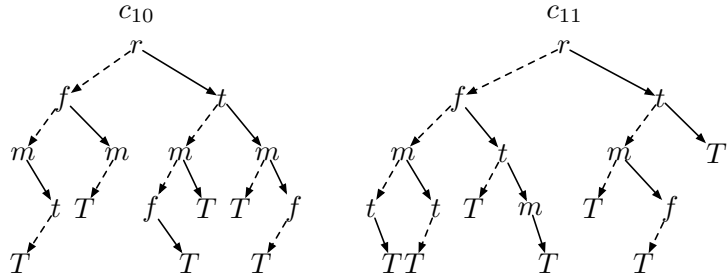
**Fig. 9.** Transfusion: logic trees for concepts c_{10} and c_{11} over essential cells, T stands for transfusion class, and a dashed line indicates a negated evaluation of the previous attribute

Table 8. Leaf paths of the first concept logic trees and their characteristics; bold numbers indicate high values

leaf path	precision	recall	accuracy	#mt	0-avg	1-avg
<i>c</i> ₁₀						
$\bar{r} \wedge \bar{f} \wedge m \wedge \bar{t}$	75%	65%	60%	1	0.049	0.047
$\bar{r} \wedge f \wedge \bar{m}$	100%	13%	39%	2	0.125	0.112
$r \wedge f \wedge \bar{m} \wedge \bar{t}$	71%	100%	72%	1	0.023	0.025
$r \wedge m \wedge \bar{t}$	83%	43%	54%	2	0.080	0.085
$r \wedge \bar{m} \wedge t$	100%	13%	39%	2	0.056	0.047
$r \wedge \bar{f} \wedge m \wedge t$	71%	100%	72%	1	0.040	0.030
<i>c</i> ₁₁						
$\bar{r} \wedge \bar{f} \wedge \bar{m} \wedge t$	73%	71%	62%	1	0.025	0.023
$\bar{r} \wedge \bar{f} \wedge m \wedge \bar{t}$	72%	64%	59%	1	0.027	0.020
$\bar{r} \wedge f \wedge \bar{t}$	67%	100%	67%	2	0.074	0.050
$\bar{r} \wedge f \wedge m \wedge t$	100%	11%	40%	1	0.271	0.193
$r \wedge \bar{m} \wedge \bar{t}$	75%	73%	66%	2	0.065	0.131
$r \wedge \bar{f} \wedge m \wedge \bar{t}$	76%	69%	64%	1	0.034	0.054
$r \wedge t$	75%	71%	64%	4	0.336	0.382

between 0-avg and 1-avg can be seen as a measure of the separation power. Notably, the third and sixth leaf paths of *c*₁₀ are interesting because their accuracy of 72% is very effective for classification.

Table 9 shows the implications between the leaf paths listed in Table 8. These implications together with Table 8 illustrate how adding minterms to a concept affects its characteristics.

Table 9. Implications between leaf paths of concepts *c*₁₀ and *c*₁₁

<i>c</i> ₁₀ leaf	implication	<i>c</i> ₁₁ leaf
$\bar{r} \wedge f \wedge m \wedge \bar{t}$	\longleftrightarrow	$\bar{r} \wedge \bar{f} \wedge m \wedge \bar{t}$
$r \wedge f \wedge \bar{m} \wedge \bar{t}$	\longrightarrow	$r \wedge \bar{m} \wedge \bar{t}$
$r \wedge m \wedge \bar{t}$	\longleftarrow	$r \wedge \bar{f} \wedge m \wedge \bar{t}$
$r \wedge \bar{m} \wedge t$	\longrightarrow	$r \wedge t$
$r \wedge \bar{f} \wedge m \wedge t$	\longrightarrow	$r \wedge t$

8 Conclusion

We addressed the problem of interpreting ANN models using logic expressions by constructing a bridge between them and visualizing these expressions as logic trees (QLDT). Thus, our interpretation method decomposes an ANN model into logic trees.

ReLU nodes in an ANN introduce non-linearity to the network, which is essential for solving non-linear classification tasks. Our approach involves partitioning a trained ANN model using ReLU conditions to obtain linear maps for each partition cell. The minterm weights of these linear maps are interpreted as bit numbers. From the resulting three-dimensional bit tensor, we apply techniques from Triadic Concept Analysis to extract triadic concepts, which are then interpreted as logic trees.

The main benefit of our approach is the ability to interpret an ANN model using logic. Logic provides a powerful toolset for analyzing how attributes interact with each other.

Our approach relies on using all minterm values as network input. Since there are 2^n minterms for n object attributes, n is restricted to be relatively small. In future work, we will strive to adapt this approach to more complex neural networks.

References

1. Balestriero, R.: Neural decision trees. arXiv preprint arXiv:1702.07360 (2017)
2. Balkenius, C., Gärdenfors, P.: Nonmonotonic inferences in neural networks. In: KR. pp. 32–39. Citeseer (1991)
3. Blutner, R.: Nonmonotonic inferences and neural networks. *Synthese* **142**, 143–174 (2004)
4. Friedman, J.H., Popescu, B.E.: Predictive learning via rule ensembles. *The Annals of Applied Statistics* **2**, 916–954 (2008), <https://api.semanticscholar.org/CorpusID:16884658>
5. Ganter, B., Wille, R.: Applied lattice theory: Formal concept analysis. Fachbereich Mathematik, Technische Hochschule Darmstadt (1997)
6. Gärdenfors, P.: How logic emerges from the dynamics of information. Lund University (1992)
7. beim Graben, P.: Incompatible implementations of physical symbol systems. *Mind and Matter* **2**(2), 29–51 (2004)
8. Granmo, O.C., Glimsdal, S., Jiao, L., Goodwin, M., Omlin, C.W., Berge, G.T.: The convolutional tsetlin machine. arXiv preprint arXiv:1905.09688 (2019)
9. Kaur, D., Uslu, S., Rittichier, K.J., Durresi, A.: Trustworthy artificial intelligence: a review. *ACM Computing Surveys (CSUR)* **55**(2), 1–38 (2022)
10. Kraus, M., Tschernutter, D., Weinzierl, S., Zschech, P.: Interpretable generalized additive neural networks. *European Journal of Operational Research* (2023)
11. Lehmann, F., Wille, R.: A triadic approach to formal concept analysis. In: Conceptual Structures: Applications, Implementation and Theory: Third International Conference on Conceptual Structures, ICCS'95 Santa Cruz, CA, USA, August 14–18, 1995 Proceedings 3. pp. 32–43. Springer (1995)
12. Lundberg, S.M., Erion, G., Chen, H., DeGrave, A., Prutkin, J.M., Nair, B., Katz, R., Himmelfarb, J., Bansal, N., Lee, S.I.: From local explanations to global understanding with explainable ai for trees. *Nature machine intelligence* **2**(1), 56–67 (2020)
13. Miller, T.: Explanation in artificial intelligence: Insights from the social sciences. *Artificial intelligence* **267**, 1–38 (2019)
14. Molnar, C.: Interpretable machine learning. Lulu. com (2020)

15. Murofushi, T., Soneda, S.: Techniques for reading fuzzy measures (iii): Interaction index. In: Proceedings of the 9th Fuzzy Systems Symposium, Sapporo. pp. 693–696 (1993)
16. Ribeiro, M.T., Singh, S., Guestrin, C.: " why should i trust you?" explaining the predictions of any classifier. In: Proceedings of the 22nd ACM SIGKDD international conference on knowledge discovery and data mining. pp. 1135–1144 (2016)
17. Roth, A.E.: Introduction to the shapley value. The Shapley value pp. 1–27 (1988)
18. Schmitt, I.: Qql: A db&ir query language. The VLDB journal **17**(1), 39–56 (2008)
19. Schmitt, I.: Incorporating weights into a quantum-logic-based query language. In: Quantum-Like Models for Information Retrieval and Decision-Making, pp. 129–143. Springer (2019)
20. Schmitt, I.: QLC: A quantum-logic-inspired classifier. In: Desai, B.C., Revesz, P.Z. (eds.) IDEAS'22: International Database Engineered Applications Symposium, Budapest, Hungary, August 22 - 24, 2022. pp. 120–127. ACM (2022). <https://doi.org/10.1145/3548785.3548790>
21. Schmitt, I.: QLDT: A decision tree based on quantum logic. In: Chiusano, S., Cerquitelli, T., Wrembel, R., Nørvåg, K., Catania, B., Vargas-Solar, G., Zumpano, E. (eds.) New Trends in Database and Information Systems - ADBIS 2022 Short Papers, Doctoral Consortium and Workshops: DOING, K-GALS, MADEISD, MegaData, SWODCH, Turin, Italy, September 5-8, 2022, Proceedings. Communications in Computer and Information Science, vol. 1652, pp. 299–308. Springer (2022). https://doi.org/10.1007/978-3-031-15743-1_28
22. Shapley, L.S., et al.: A value for n-person games. Princeton University Press Princeton (1953)
23. Suthaharan, S., Suthaharan, S.: Decision tree learning. Machine Learning Models and Algorithms for Big Data Classification: Thinking with Examples for Effective Learning pp. 237–269 (2016)
24. Wei, L., Qian, T., Wan, Q., Qi, J.: A research summary about triadic concept analysis. International Journal of Machine Learning and Cybernetics **9**, 699–712 (2018)
25. Yang, Y., Morillo, I.G., Hospedales, T.M.: Deep neural decision trees. arXiv preprint arXiv:1806.06988 (2018)